

## Distributed Prony analysis for real-world PMU data

Javad Khazaei<sup>a</sup>, Lingling Fan<sup>a,\*</sup>, Weiqing Jiang<sup>b</sup>, Durgesh Manjure<sup>b</sup>

<sup>a</sup> Department of Electrical Engineering, University of South Florida, Tampa, FL 33620, USA

<sup>b</sup> MISO Energy, 720 City Center Drive, Carmel, IN 46302, USA



### ARTICLE INFO

#### Article history:

Received 1 July 2015

Received in revised form 6 November 2015

Accepted 9 December 2015

#### Keywords:

Prony analysis

PMU data

Distributed optimization

### ABSTRACT

Prony analysis has been applied in power system oscillation identification for decades. For a single PMU signal with 30 Hz sampling rate, merely applying Prony analysis cannot give accurate results of oscillating modes of power systems. This paper presents an analysis to show the effect of sampling rate on estimation accuracy and the mitigation methods to obtain accurate estimation. The methods include sampling rate reduction and multiple-signal Prony analysis. For multiple-signal Prony analysis, this paper proposes a distributed Prony analysis algorithm using consensus and subgradient update. This algorithm can be applied to multiple signals from multiple locations collected at the same period of time. This algorithm is scalable and can handle a large-dimension of PMU data by solving least square estimation problems with small sizes in parallel and iteratively. Real-world PMU data are used for analysis and validation. The proposed distributed Prony analysis shows being robust against sampling rate and generates reconstructed signals with better matching degree compared to the conventional Prony analysis for multiple signals.

© 2015 Elsevier B.V. All rights reserved.

### 1. Introduction

A power system is a massive system that can be perturbed by load changes, generator trips, faults or networks changes. Power system oscillations are common issues. To mitigate oscillations, oscillations should be identified and studied in a timely manner. There are two separate approaches to identify power system oscillations. The first approach is based on detailed dynamic model of the system such as: eigenvalue analysis or state space modeling [1]. Detailed modeling of a huge complicated power system is challenging and prone to errors. The second approach is based on measurements to identify oscillation modes. Measurement-based approach has been adopted by control engineers in practice. For example, equivalent system models will be constructed based on the measurement and further control strategies will be developed based on the identified system models.

With phasor measurement unit (PMU) data collected, electromechanical oscillation modes can be identified from these measurements. Several measurement-based system identification have been proposed for PMU data-based estimation, such as Kalman filters [2–4], least square estimation [5], and subspace algorithm [6]. Prony analysis is one of the most common

measurement-based identification approaches to identify oscillatory modes. Prony analysis has been introduced by Hauer *et al* in power systems in 1990 [7,8]. The main idea is to directly estimate the frequency, damping and phase of modal components of a measured signal. An extension to Prony analysis is then introduced which allowed multiple signals to be analyzed at the same time resulting in one set of oscillatory modes [9].

Since then, Prony analysis has been applied in power system oscillation identification for decades. For PMU data with 30 Hz sampling rate, it is found that merely applying Prony analysis cannot give accurate results of oscillating modes of power systems. Zhou *et al.* have identified this issue in [10,11] and provided a solution. By re-sampling the PMU data to a lower sampling rate, the estimation will be more accurate. In this paper, an analysis is presented to show the effect of sampling rate on accuracy.

Mitigation methods are also presented in this paper to obtain accurate estimation. The two mitigation methods investigated include sampling rate reduction and multiple-signal Prony analysis. For multiple-signal Prony analysis, scalability is an issue given the large size of PMU data. A distributed algorithm is proposed in this paper to handle the issue of scalability. The objective of the algorithm is to have multiple Phasor Data Centers (PDCs) to conduct estimation at the same time. These PDCs will only utilize the local PMU data with limited information exchange from other PDCs. The computation effort is thus drastically reduced for each computing agent.

\* Corresponding author. Tel.: +1 813 974 2031; fax: +1 813 974 5250.  
E-mail address: [linglingfan@usf.edu](mailto:linglingfan@usf.edu) (L. Fan).

Application of distributed optimization techniques has recently been introduced in system modes identification [12–14]. For example, in [12], distributed Prony analysis using alternating direction method of multipliers (ADMM) has been combined with centralized Prony method to estimate the slow frequency eigenvalues. Simulation data generated by PST [15] toolbox of IEEE 39-bus system is used to conduct Prony analysis.

While [13,12] have discussed the ADMM implementation, many details on Prony analysis have not been elaborated, e.g., sampling rate effect and validation through signal reconstruction. Further, the PMU data in [13] come from computer simulation. In this paper, real-world PMU data from Eastern Interconnection will be used for tests. The real-world PMU data has more complex characteristics.

This paper will develop a distributed Prony analysis algorithm using consensus and subgradient update. This algorithm can be applied to multiple signals from multiple locations collected the same period of time. This algorithm can handle a large-dimension of PMU data by solving least square estimation (LSE) problems with small sizes in parallel and iteratively. Moreover, convergence analysis is carried out to examine convergence. Robustness of the algorithm against sampling rate will also be examined. The rest of the paper is as follows: Section 2 describes the fundamentals of Prony analysis. An analysis of effect of sampling rate on estimation is presented in Section 3. Distributed Prony analysis including the general description and convergence analysis is described in Section 4. Section 5 presents case study results. Conclusion is presented in Section 6.

## 2. Fundamentals of Prony analysis

Consider a Linear-Time Invariant (LTI) system with the initial state of  $x(t_0)=x_0$  at the time  $t_0$ , if the input is removed from the system, the dynamic system model can be represented as [16]:

$$\dot{x}(t) = Ax(t) \quad (1)$$

$$y(t) = Cx(t) \quad (2)$$

where  $y \in \mathbb{R}$  is defined as the output of the system,  $x \in \mathbb{R}^n$  is the state of the system,  $A \in \mathbb{R}^{n \times n}$  and  $C \in \mathbb{R}^{1 \times n}$  are system matrices. The order of the system is defined by  $n$ . If the  $\lambda_i$ ,  $p_i$ , and  $q_i$  are the  $i$ -th eigenvalues, right eigenvectors, and left eigenvectors of  $n \times n$  matrix  $A$ , respectively, the (1) can be solved as:

$$\begin{aligned} x(t) &= \sum_{i=1}^n (q_i^T x_0) p_i e^{\lambda_i t} \\ &= \sum_{i=1}^n R_i x_0 e^{\lambda_i t} \end{aligned} \quad (3)$$

where  $x_0$  is the initial state and  $R_i = p_i q_i^T$  is a residue matrix. Based on (2), the  $y(t)$  can be expressed as:

$$y(t) = \sum_{i=1}^n C R_i x_0 e^{\lambda_i t}. \quad (4)$$

Prony analysis directly estimates the parameters for the exponential terms in (4) by defining a fitting function in a basic form of:

$$\hat{y}(t) = \sum_{i=1}^n B_i e^{\sigma_i t} \cos(2\pi f_i t + \varphi_i) \quad (5)$$

The observed or measured  $y(t)$  consists of  $N$  samples which are equally spaced by  $\Delta t$  as:  $y(t_k)=y(k)$ ,  $k=1, \dots, N-1$ . The basic assumption is to consider the signal record to be noise free and

the order of the system can be set as:  $n=N/2$  [7]. Therefore, (5) can be recast in the exponential form as:

$$\begin{aligned} \hat{y}(t_k) &= \Re \left( \sum_{i=1}^n B_i e^{\lambda_i k \Delta t} \right) \\ &= \Re \left( \sum_{i=1}^n B_i z_i^k \right), \quad k = 1, \dots, N \end{aligned} \quad (6)$$

where  $N$  is the number of samples,  $z_i$  are the eigenvalues of the system in discrete time domain, and  $B_i$  is the residue of  $z_i$ .  $z_i$  can be expressed as:

$$z_i = e^{\lambda_i \Delta t} \quad (7)$$

Due to the fact that  $k = 1, \dots, N$ , (6) can be expressed in matrix form as:

$$\begin{bmatrix} B_1 z_1^0 + \dots + B_n z_n^0 \\ B_1 z_1^1 + \dots + B_n z_n^1 \\ \vdots \\ B_1 z_1^{N-1} + \dots + B_n z_n^{N-1} \end{bmatrix} = \begin{bmatrix} y(0) \\ y(1) \\ \vdots \\ y(N-1) \end{bmatrix}. \quad (8)$$

Or in a simple form:  $ZB=Y$  as shown in (9).

$$\begin{bmatrix} z_1^0 & z_2^0 & \dots & z_n^0 \\ z_1^1 & z_2^1 & \dots & z_n^1 \\ \vdots & \vdots & \vdots & \vdots \\ z_1^{N-1} & z_2^{N-1} & \dots & z_n^{N-1} \end{bmatrix} \begin{bmatrix} B_1 \\ B_2 \\ \vdots \\ B_n \end{bmatrix} = \begin{bmatrix} y(0) \\ y(1) \\ \vdots \\ y(N-1) \end{bmatrix} \quad (9)$$

As the  $z_i$  are the roots of the characteristic polynomial function of the system, in order to find the  $z_i$ , the coefficients of the polynomial need to be found first. The polynomial is formed as:

$$z^n - (a_1 z^{n-1} + a_2 z^{n-2} + \dots + a_n z^0) = 0. \quad (10)$$

While the roots  $z_i$  might be complex numbers, the system polynomial coefficients  $a_i$  are real numbers. This feature helps develop algorithms since real numbers will be handled by computer algorithms while complex numbers cannot be directly handled.

From (10), we have

$$z^n = a_1 z^{n-1} + a_2 z^{n-2} + \dots + a_n z^0. \quad (11)$$

Further, a linear prediction model (12) can be formulated since  $y(k)$  is the linear combination of  $z_i(k)$  based on (6). Therefore,

$$y(n) = a_1 y(n-1) + a_2 y(n-2) + \dots + a_n y(0). \quad (12)$$

Enumerate the signal samples from  $n$  step to  $N$  step, we have (13):  $Y=Da$ .

$$\underbrace{\begin{bmatrix} y(n) \\ \vdots \\ y(n+k) \\ \vdots \\ y(N) \end{bmatrix}}_Y = \underbrace{\begin{bmatrix} y(n-1) & y(n-2) & \dots & y(0) \\ \vdots & \vdots & \ddots & \vdots \\ y(n+k-1) & y(n+k-2) & \dots & y(k) \\ \vdots & \vdots & \ddots & \vdots \\ y(N-1) & y(N-2) & \dots & y(N-n) \end{bmatrix}}_D \underbrace{\begin{bmatrix} a(1) \\ \vdots \\ a(k) \\ \vdots \\ a(n) \end{bmatrix}}_a \quad (13)$$

*Remarks:* The dimension of  $D$  matrix is  $N-n+1$ ,  $n$ . If  $n < N/2$ , this is an over-determined linear equation and will be solved by the least square estimation (LSE). If  $n > N/2$ , the linear equations are under-determined and there are multiple solutions for  $a$ . When the  $D$  matrix is square, there is a unique solution of  $a$  and the match will be the best for. That is the reason that  $n$  is selected to be close to  $N/2$  [7].

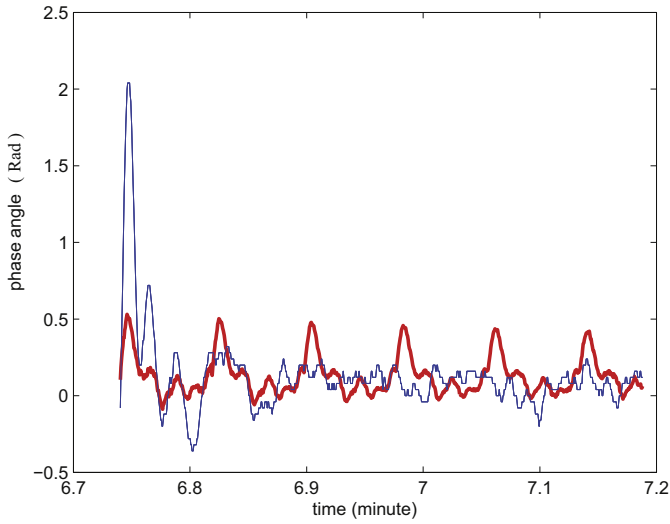


**Fig. 1.** Reconstructed signal versus PMU measurement for 30 s. Sampling rate 30 Hz. Blue: measurement. Red: reconstructed signal. (For interpretation of the references to color in this figure legend, the reader is referred to the web version of this article.)

Briefly,  $Da = Y$  will be obtained, where  $a$  contains the coefficients of the characteristic polynomial (10) of the system and  $D$  and  $Y$  are constructed from the measured signals. Solution of (13) will provide the coefficients of (10). From (10), the roots  $z_i$  ( $i = 1, \dots, n$ ) will be found.

The next step of the Prony analysis is to find the residues  $B_i$  in (6). As a result,  $B_i$  can be found by solving a set of overdetermined linear equations (9).

### 2.1. Signal reconstruction

Equation (9) can also be used to reconstruct the estimated signals. For a given set of residues  $B_i$  and system roots  $z_i$ , signals at every sample can be found.

### 3. Effect of sampling rate

For PMU data with 30 Hz sampling rate, Prony analysis cannot give a good match. Fig. 1 presents the comparison of the reconstructed signal and the PMU measurement. The sampling rate of the signal is 30 Hz. It can be observed that the degree of match is poor. The reconstructed signal (thick line) has some undamped modes presented like harmonics. The identified eigenvalues are computed and listed in Table 1. It can be seen that all modes have very poor damping.

The identified system roots  $z_i$  are shown in Fig. 2. It can be seen that the roots are all located on the unit circle.

One reason for inaccuracy in estimation is related to the issue of outfitting. With a high sampling rate, there will be more data samples. In Prony analysis, the order of the system is chosen to be half of the number of samples. For example, at 30 Hz sampling rate, for 30 s data, we end up estimating a 450-order system or

**Table 1**  
Identified eigenvalues with 30 Hz sampling rate.

Real part	Mode frequency (Hz)	Residue
-0.0343	1.3980	0.0131
-0.0016	0	0.129
-0.0157	0.7989	0.0381
-0.0087	0.5996	0.0243
-0.0084	0.1991	0.0766
-0.0092	0.4009	0.0453

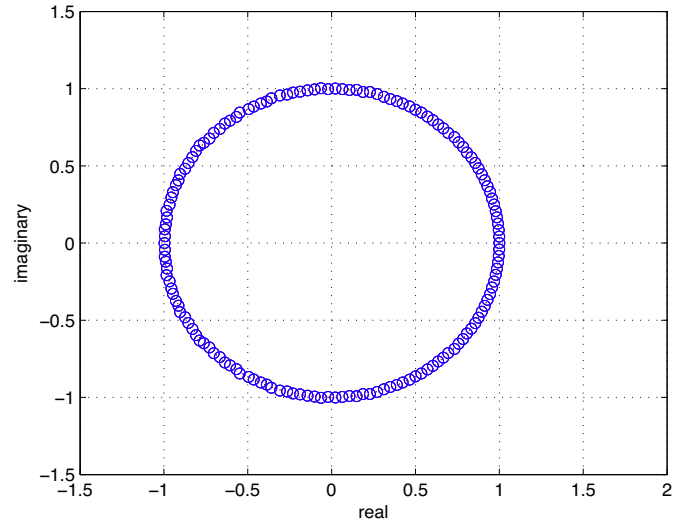


**Fig. 2.** System roots in Z-plane. Sampling rate 30 Hz.

approximately 450 parameters. In machine learning or data fitting, this is a known issue as overfitting when the number of parameters or features increases [17]. The fitting process tries to adjust parameters to fit signals with noise realization. Reducing sampling rate is similar as taking averaging and reducing noise effect. Therefore, a lower sampling rate can improve accuracy of estimation. Zhou et al. have identified this issue in [11] and provided a solution. By re-sampling the PMU data to a lower sampling rate, the estimation will be more accurate. This section will perform an analysis to show the second reason of inaccuracy: numerical error.

### 3.1. Analysis

Note that the dominant system roots  $z_i$  are related to the dominant eigenvalue  $\lambda_i$  as follow.

$$z_i = e^{\lambda_i T} \tag{14}$$

where  $T$  is the sampling period. With the assumption that the damping of the dominant mode is negligible, then  $\lambda_i \approx j\omega_i$  and  $|z_i| \approx 1$ .

$$\begin{aligned} \lambda_i &\approx j\omega_i = \frac{\log z_i}{T} = \frac{\log |z_i| e^{j\theta_i}}{T} = \frac{\log |z_i| + j\theta_i}{T} \\ &\approx j \frac{\theta_i}{T} \end{aligned} \tag{15}$$

where  $\theta_i$  is the angle of  $z_i$  on the Z-plane. Therefore

$$\theta_i = \omega_i T. \tag{16}$$

Suppose the dominant mode of the power system is 0.2 Hz, for 30 Hz sampling rate,  $T = 1/30$ s, it can be found that the dominating root's angle in Z-plane is 2.4 degree. When the sampling rate is 5 Hz,  $\theta = 14$  degree. A 5 Hz sampling rate will make the Prony analysis more accurate since the real part  $|z_i| \cos \theta_i$  and imaginary part  $|z_i| \sin \theta_i$  are relatively comparable. For a 30 Hz sampling rate,  $|z_i| \cos \theta_i \approx 1$  and  $|z_i| \sin \theta_i \approx 0$ , it is more prone to numerical error in identification.

For the sample signal presented in Fig. 1, the signal is resampled to have a 6 Hz sampling rate. The dominating  $z_i$  for the two cases are compared in Table 2. It can be seen that that for 30 Hz case, the real parts of the system roots are all close to 1, while for the 6 Hz case, the real parts of the system roots are dispersed.

The system roots for 6 Hz sampling rate are shown in Fig. 3. It can be observed that the system roots are more dispersed around the unit circle. The corresponding eigenvalues are shown in Table 3.

**Table 2**  
Comparison of dominating  $z_i$  for 30 Hz and 6 Hz sampling rate.

Z: real + imag
0.9563 + 0.2883i
0.9563 - 0.2883i
0.9999
0.9855 + 0.1665i
0.9855 - 0.1665i
0.9918 + 0.1252i
0.9918 - 0.1252i
0.9988 + 0.0417i
0.9988 - 0.0417i
0.9962 + 0.0838i
0.9962 - 0.0838i
Z: real + imag
0.8094 + 0.5074i
0.8094 - 0.5074i
-0.5597 + 0.7476i
-0.5597 - 0.7476i
-0.8203 + 0.3191i
-0.8203 - 0.3191i
-0.4685 + 0.6841i
-0.4685 - 0.6841i
0.6210
0.2271

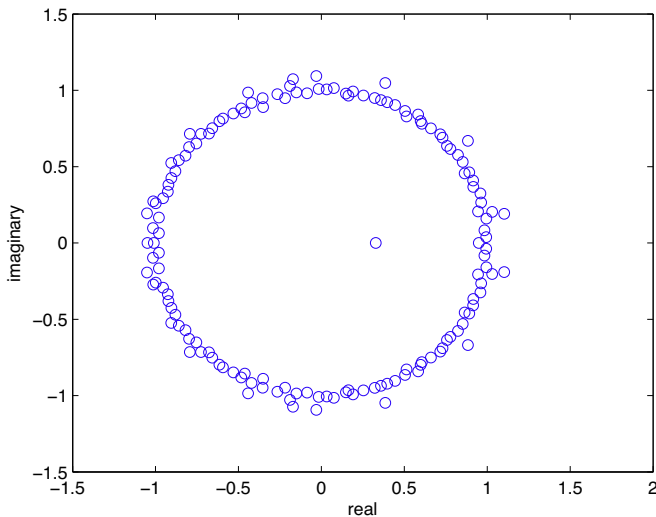


**Fig. 3.** System roots in Z-plane. Sampling rate 6 Hz.

One dominating mode is of 0.44 Hz. The reconstructed signal has a better matching degree as shown in Fig. 4 compared to the previous reconstructed signal shown in Fig. 1.

The above analysis examines eigenvalue locations for a discrete system and draws conclusion that a lower sampling rate provides better identification for dominant mode. Reducing sampling rate also significantly reduces higher frequency noise. Therefore, the benefit of a reduced sampling rate on more accurate mode

**Table 3**  
Identified eigenvalues with 6 Hz sampling rate.

Real part	Mode frequency (Hz)	Residue
-0.2284	0.4456 Hz	0.2226
-0.3416	1.7614 Hz	0.2779
-0.6381	2.2048 Hz	0.4944
-0.9370	1.7279 Hz	1.0691
-2.3818	8.5916	
-7.412	11.595	

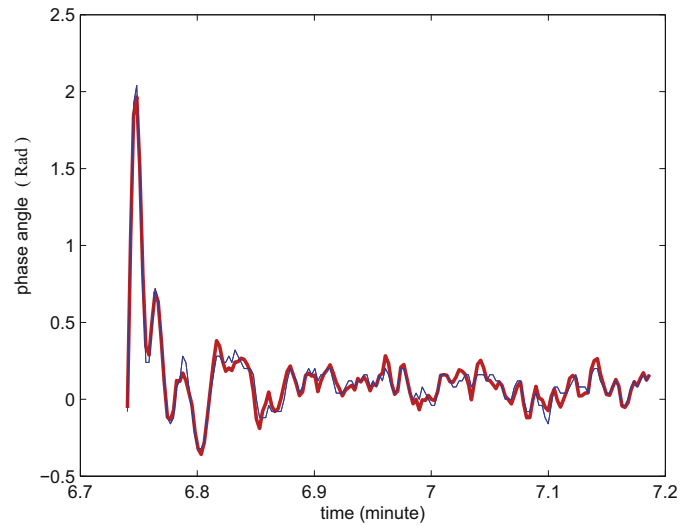


**Fig. 4.** Reconstructed signal versus PMU measurement for 30 s. Sampling rate: 6 Hz. Blue: measurement. Red: reconstructed signal. (For interpretation of the references to color in this figure legend, the reader is referred to the web version of this article.)

identification can be explained by reduced impact of numerical error and reduced noise components.

#### 4. Distributed Prony analysis

Section 2 discusses the case where signals from one channel are used for the Prony analysis. In reality, each PMU provides multiple signal channels and a control center may collect PMU data from hundreds or thousands of PDCs. The PMU data from multiple PDCs should contain the same system modes, although different measurements have different residues or observability for a certain mode.

The conventional way to find the vector  $a$  from multiple signals has been documented in [9]. A brief description is offered as follows. Suppose that there are  $m$  channels of PMU data taken from the same period of time. For each channel of the PMU data, it is possible to formulate the  $D$  matrix and  $Y$  vector. They will be notated as  $D_i$  and  $Y_i$  for the  $i$ -th channel.  $a$  can be found by the following equation:

$$\begin{bmatrix} D_1 \\ D_2 \\ \vdots \\ D_m \end{bmatrix} a = \begin{bmatrix} Y_1 \\ Y_2 \\ \vdots \\ Y_m \end{bmatrix} \quad (17)$$

Indicated in [9], the more measurements, Prony analysis will be more accurate. This is due to the fact that to make the estimation of a single signal accurate, the Prony analysis adopts a high system order to make  $D_i$  matrix almost square. The noise in that signal will be included in the system model. By considering multiple signals, the effect of noise in one signal will be evened out. Therefore, case studies in [9] show significant improvement in modal estimation by using multiple signals.

To achieve scalability, in this section, a distributed Prony analysis method is proposed using distributed optimization techniques. When the number of the signal channels increases, the least square estimation has to handle a large dimension of matrix. The size of the matrix will be tremendous if a long period of time with signals collected from thousands of locations is considered. Therefore, in this section, the original nonconstrained optimization problem will be converted to a consensus problem. Consensus and subgradient update approach will be adopted to conduct Prony analysis.

Prony analysis is to identify system polynomials from the signals. Suppose there are two channels of signals to be dealt with and the dimension of  $a$  vector is 1. The optimization problem is

$$\min_a \|D_1 a - Y_1\|_2^2 + \|D_2 a - Y_2\|_2^2 \quad (18)$$

The above problem can be converted to a consensus problem as:

$$\min_{b_1, b_2} \|D_1 b_1 - Y_1\|_2^2 + \|D_2 b_2 - Y_2\|_2^2 \quad (19)$$

$$\text{subject to } b_1 = b_2 \quad (20)$$

The objective function can be decomposed into two objective functions each related to  $b_i$  only. Therefore, two subproblems will be solved:

$$\min_{b_i} \|D_i b_i - Y_i\|_2^2 \quad (21)$$

The two subproblems need to have a consensus solution. To achieve this objective, an iterative approach with consensus update and subgradient update is adopted [18]. The consensus update is to guarantee that  $b_1 = b_2$  while the subgradient update guarantees that the update direction decreases the objective function.

$$\begin{aligned} b_1(k+1) &= 0.5b_1(k) + 0.5b_2(k) - \alpha D_1^T (D_1 b_1(k) - y_1) \\ b_2(k+1) &= 0.5b_1(k) + 0.5b_2(k) - \alpha D_2^T (D_2 b_2(k) - y_2) \end{aligned} \quad (22)$$

Extend the formulation to  $m$  signals and the dimension of the system order is  $n_p$ , then the update equation for each  $z_i$  will be as follows.

$$b_i(k+1) = M \sum_{i=1}^m b_i(k) - \alpha D_i^T (D_i b_i(k) - Y_i) \quad (23)$$

where  $b_i \in \mathbb{R}^{n_p}$ ,  $M$  is a diagonal matrix with a dimension of  $n_p \times n_p$ . For  $j$ -th element of  $b_i$ , the consensus part of the update (without the subgradient update) is as follows.

$$b_{ji}(k+1) = \begin{bmatrix} M_{jj} & M_{jj} & \cdots & M_{jj} \end{bmatrix} \begin{bmatrix} b_{j1}(k) \\ b_{j2}(k) \\ \vdots \\ b_{jm}(k) \end{bmatrix} \quad (24)$$

For the  $j$ -th element of all  $m$  signals, the vector format of the update is as follows.

$$\begin{bmatrix} b_{j1}(k+1) \\ b_{j2}(k+1) \\ \vdots \\ b_{jm}(k+1) \end{bmatrix} = \underbrace{\begin{bmatrix} M_{jj} & M_{jj} & \cdots & M_{jj} \\ M_{jj} & M_{jj} & \cdots & M_{jj} \\ \vdots & \vdots & \ddots & \vdots \\ M_{jj} & M_{jj} & \cdots & M_{jj} \end{bmatrix}}_{M_M} \begin{bmatrix} b_{j1}(k) \\ b_{j2}(k) \\ \vdots \\ b_{jm}(k) \end{bmatrix} \quad (25)$$

To have a converged consensus update, the matrix  $M_M$  should be a Markov stochastic matrix [18], or the sum of its row should be 1 and each element should be greater or equal zero. The element of  $M_M$  can be selected as  $1/m$  to meet the requirement.

#### 4.1. Convergence analysis

For subgradient update,  $\alpha$  has to be small enough to guarantee convergence [19]. In this paragraph, a simple example will be used to demonstrate  $\alpha$  versus convergence.

For two signals  $y(t) = e^{-2t}$  and  $y(t) = e^{2t}$ , the samples from 0 to 2 s with a sampling rate as 0.01 s are obtained. Then the system

polynomial is  $y(n) - ay(n-1) = 0$  where  $a^* = e^{-0.02}$  or  $a^* = e^{0.02}$ . The matrix and vector constructed for estimation are:

$$D = \begin{bmatrix} y(0) \\ y(1) \\ \vdots \\ y(N-1) \end{bmatrix}, Y = \begin{bmatrix} y(1) \\ y(2) \\ \vdots \\ y(N) \end{bmatrix} = Da \quad (26)$$

Therefore, the subgradient update equation becomes:

$$a(k+1) = a(k) - \alpha D^T (Da(k) - y) \quad (27)$$

$$= a(k) - \alpha D^T D (a(k) - a^*) \quad (28)$$

$$= (1 - \alpha D^T D) a(k) + \alpha D^T a^* \quad (29)$$

$$D^T D = \sum_{i=0}^{N-1} y^2(i) \quad (30)$$

To have a convergence sequence of  $a$ , the absolute value of the coefficient of  $a(k)$  in the above equation should be less than 1. For the two signals,  $e^{-2t}$  and  $e^{2t}$ ,  $D^T D$  of the former signal is much smaller than that of the latter signal.

$$|1 - \alpha D^T D| < 1 \quad (31)$$

Therefore,  $\alpha$  for the second signal should be much smaller than the first signal. Fig. 5(a) and 5(b) presents two convergent cases of identifying  $a$  for the two signals. Note that the first case has an  $\alpha = 10^{-4}$  while the latter case has an  $\alpha = 10^{-6}$ .

### 5. Case study and numerical results

Six real-world PMU signals with a 3 Hz sampling rate are used to demonstrate the distributed Prony analysis. These signals come from East Interconnection and are shown in Fig. 6. Note that one of the signals (signal 3) has significant noise since voltage magnitude in general should be much more smooth. The time duration is about 0.47 min or 28 s. The number of the samples for each signal is 854. With the signals resampled to have a 6 Hz sampling rate, the number of the samples is 170.

Based on the 6 Hz sampled signals, three types of Prony analysis are conducted: (1) Prony analysis based on individual signal. Since the number of the samples is 170, the order of the system is chosen to be 85 and 85 polynomial coefficients will be estimated; (2) distributed Prony based on (23). The step size  $\alpha$  is selected as 0.00002; and (3) Prony analysis based on multiple signals using (17).

Fig. 7 presents the 85 polynomial coefficients for 30 iterations. It can be observed that after 30 iterations, the 85 coefficients are converging to constants. Using these coefficients ( $a_i$ ), the roots of the system in (11) can be found which in turn leads to the finding of the eigenvalues  $\lambda_i$  (3). Further, the residues  $B_i$  in (6) can be found based on (9). Using the aforementioned information, signals will be reconstructed and examined for their matching degree with the original signals.

Figs. 8–10 present the comparison of the three types of Prony analysis results. Fig. 8 presents a comparison of the reconstructed signal 1 based on the three methods. Fig. 9 provides a zoomed-in picture. Fig. 10 presents a comparison for Signal 5. It can be seen that the performance of distributed Prony analysis is comparable or better than the multi-signal Prony analysis. In addition, for each signal and its reconstructed signal, the errors are recorded. Table 4 presents the sum of error squares for each method. Table 5 presents the ratio of the sum of error squares over the sum of the signal squares. It can be found that distributed Prony analysis has the least total error square while Prony analysis employing multiple signals leads to the largest total error square. Also based on visual observation from Figs. 8–10, distributed Prony-based

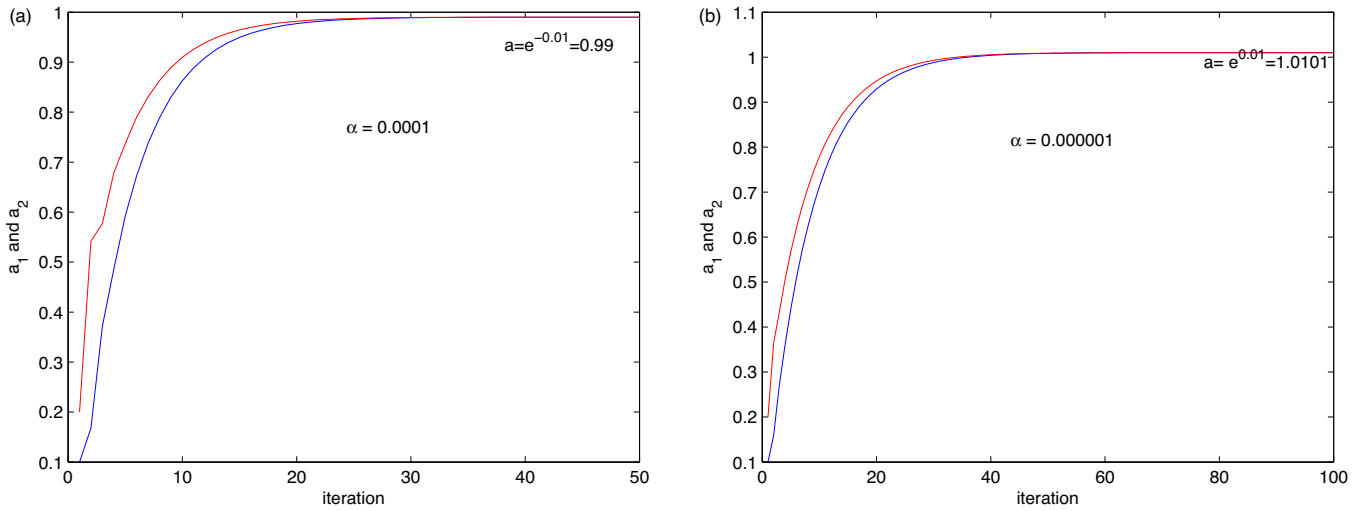


Fig. 5. (a) System polynomial coefficient estimation for  $2e^{-t}$  and  $10e^{-t}$ ; (b)  $2e^t$  and  $10e^t$ . Blue:  $a_1$ . Red:  $a_2$ . (For interpretation of the references to color in this figure legend, the reader is referred to the web version of this article.)

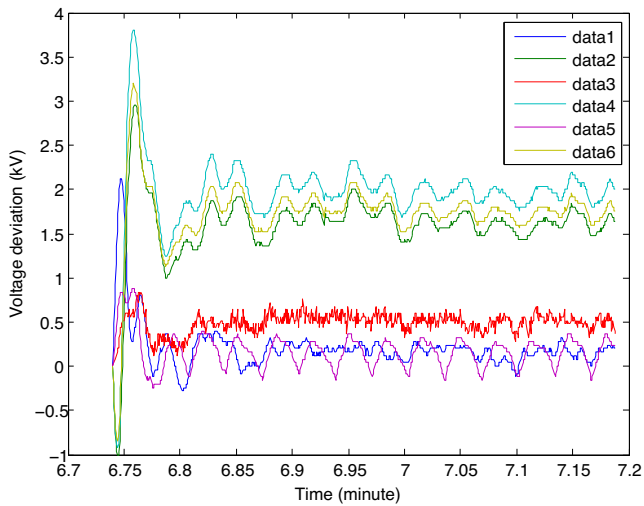


Fig. 6. Six voltage deviation signals for 30s.

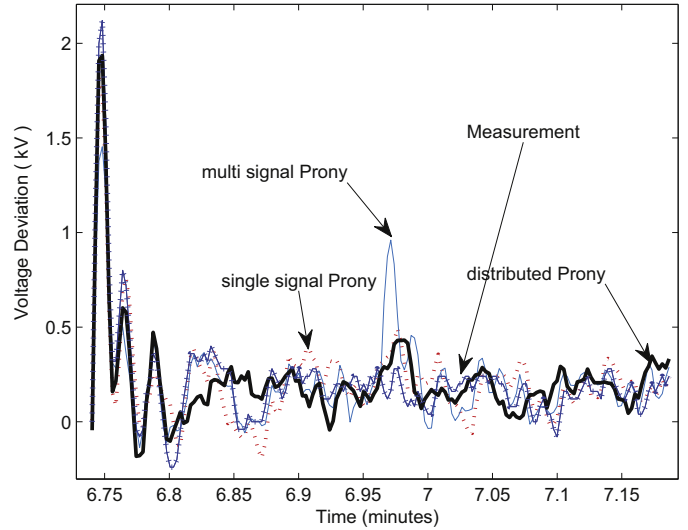


Fig. 8. Reconstructed Signal 1 comparison.

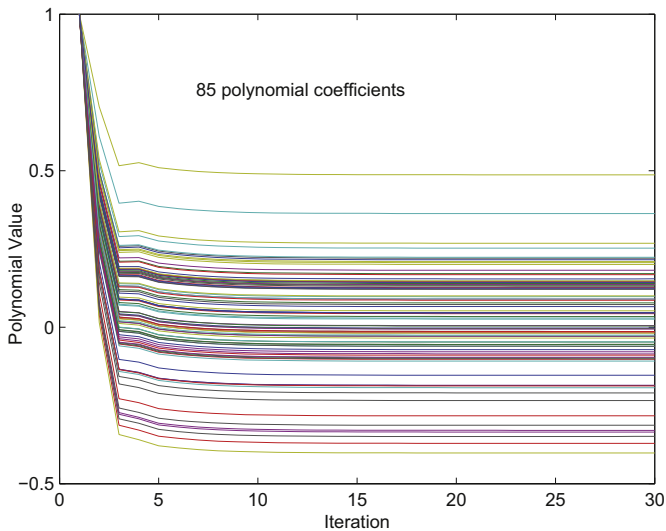


Fig. 7. Iteration to compute 85 polynomial coefficients.

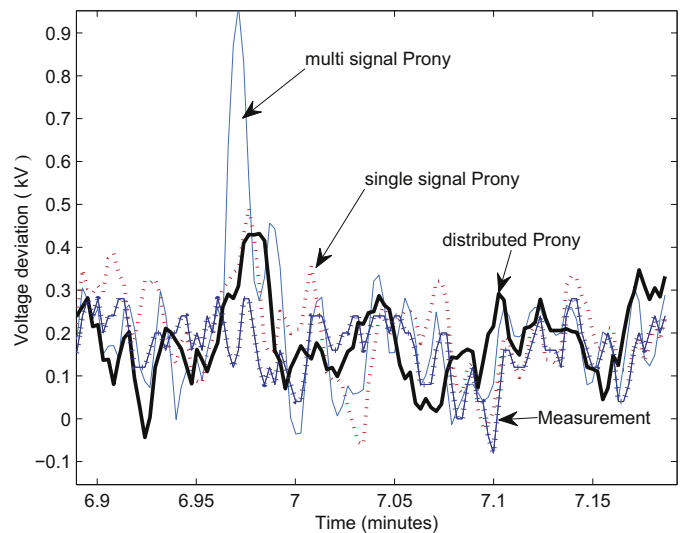


Fig. 9. Reconstructed Signal 1 comparison for 30s.

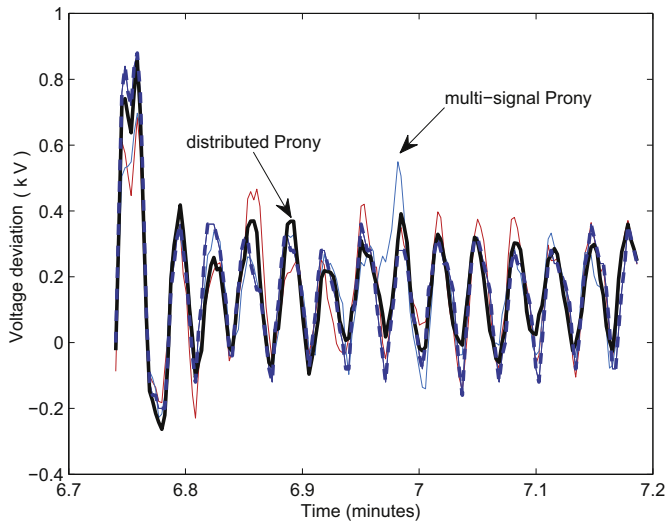


Fig. 10. Reconstructed Signal 5 comparison for 30 s.

reconstruction and single-signal Prony-based reconstruction show high matching degree. The multi-signal Prony-based reconstruction shows the worst matching degree. One reason is that with multiple signals, signals are in different scales and the noises have different deviation. When they are treated with the same weight, the estimation deviates from the true value. In distributed Prony analysis, the set of the parameters is estimated to try to minimize the error square for individual signal. The solving procedures for a weighted least square estimation (LSE) and non-weighted LSE are the same. Therefore, in distributed Prony analysis, difference in signal noise variations is automatically counted. This feature leads to more accurate estimation and better matching degree for reconstructed signals.

5.1. Robustness against sampling rate

In this section, distributed Prony analysis and multi-signal Prony analysis are conducted for 30 Hz sampling rate. Each signal has 854

Table 4  
Sum of error square for each method.

	Single-signal Prony	Distributed Prony	Multi-signal Prony
Signal 1	2.4991	2.3673	4.5024
Signal 2	2.3997	2.6547	9.4983
Signal 3	0.8713	0.7334	0.9200
Signal 4	5.1504	3.0354	12.0500
Signal 5	1.4722	0.8084	1.6397
Signal 6	1.5485	2.2459	9.0145
Sum	13.9413	11.7374	37.6248

Table 5  
Percentage sum of error square for each method.

	Single-signal Prony	Distributed Prony	Multi-signal Prony
Signal 1	11.88	12.48	21.39
Signal 2	0.51	0.60	2.03
Signal 3	2.00	1.80	2.11
Signal 4	0.74	0.48	1.72
Signal 5	12.97	6.98	14.44
Signal 6	0.28	0.46	1.66

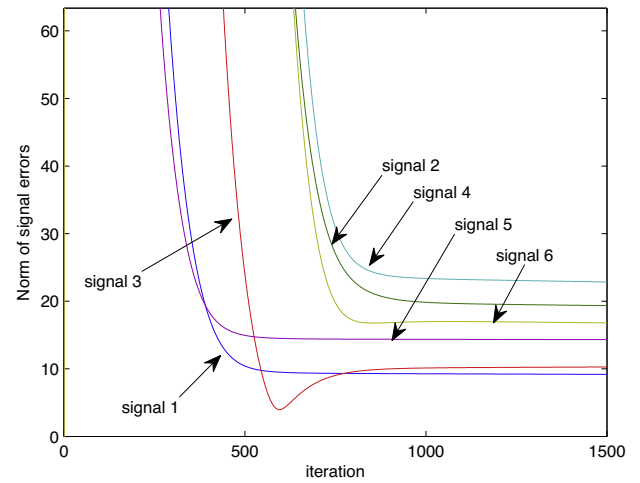


Fig. 11. The norms of the subgradients  $\|D_i^T(D_i b_i - Y_i)\|_2$ .

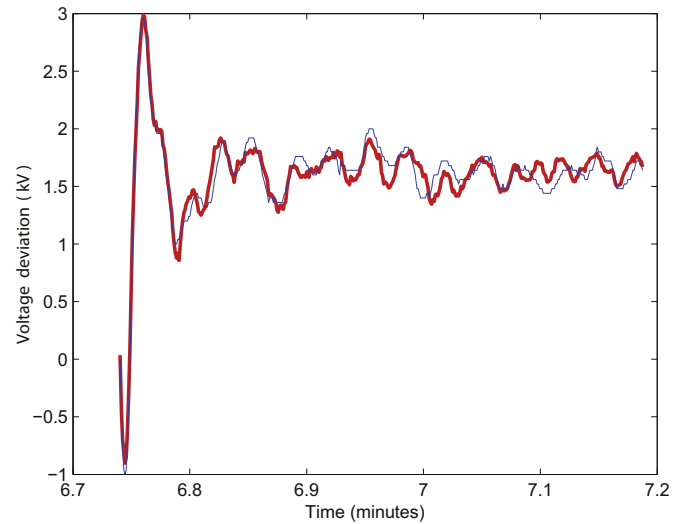
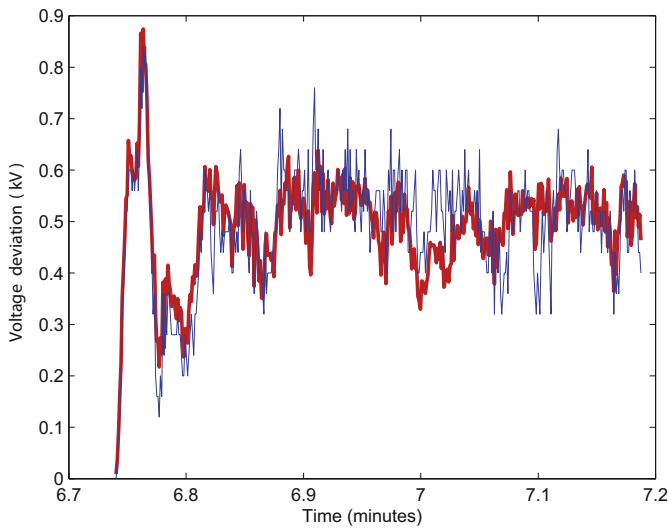


Fig. 12. Reconstructed signal 2 based on Prony analysis results for 30 s. Blue: measurement. Red: reconstructed signal. (For interpretation of the references to color in this figure legend, the reader is referred to the web version of this article.)

samples and the system order is 427. For this analysis, the step size  $\alpha$  is chosen as  $10^{-7}$  to have a convergent case. When  $\alpha$  is chosen as  $10^{-5}$ , the iteration is not converging. It is found that when multiple signals are considered, the estimation at the original sampling rate is also accurate. This is due to the fact that noises presented in one signal will not have a significant impact on estimation.

The norms of the subgradients for the six signals during the iteration step are plotted in Fig. 11. The subgradients have not reached zero. However, given that the step size  $\alpha$  is very small, their product can be considered as negligible. Therefore, after 1500 iteration, the minimum of  $\|D_i a_i - Y_i\|$  achieves.

Three signals are selected to show the degree of match between reconstructed signal and the measurement signal as shown in Figs. 12–14. A high degree of match is found. A comparison of error square sum is presented in Table 6 where reconstructed signals based on 6 or 30 Hz distributed Prony analysis are compared for their matching degree. It shows that using 30 Hz sampling rate provides a comparable matching degree as using 6 Hz sampling rate. This observation confirms the previous remarks on distributed Prony analysis that it works as weighted LSE automatically.



**Fig. 13.** Reconstructed signal 3 based on Prony analysis results for 30 s. Blue: measurement. Red: reconstructed signal. (For interpretation of the references to color in this figure legend, the reader is referred to the web version of this article.)

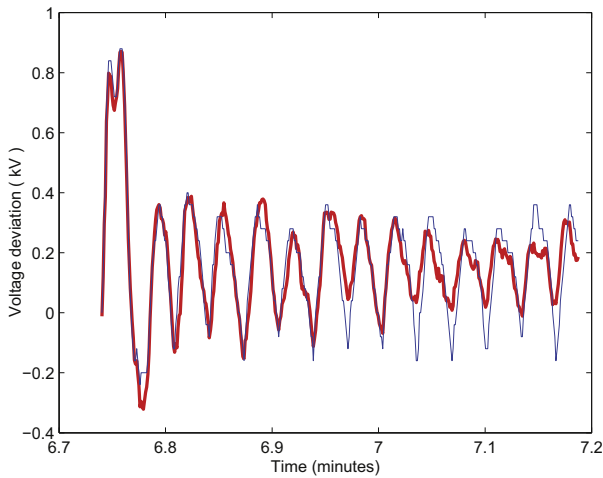


**Fig. 14.** Reconstructed signal 5 based on Prony analysis results for 30 s. Blue: measurement. Red: reconstructed signal. (For interpretation of the references to color in this figure legend, the reader is referred to the web version of this article.)

**Table 6**

Percentage sum of error square for each method.

	30 Hz distributed Prony	6 Hz distributed Prony	30 Hz multi-Prony	6 Hz multi-Prony
Signal 1	11.94	12.48	28.74	21.39
Signal 2	0.93	0.60	2.85	2.03
Signal 3	1.50	1.80	2.38	2.11
Signal 4	0.77	0.48	2.44	1.72
Signal 5	6.21	6.98	20.26	14.44
Signal 6	0.74	0.46	2.31	1.66

## 6. Conclusion

This paper analyzed the impact of sampling rate on power system modal detection using Prony analysis. Further, the paper

presents a distributed Prony analysis method using consensus and subgradient update. The algorithm can be applied on multiple-signals Prony analysis. At each iteration, small-size subproblems are dealt with in parallel. The procedure of the implementation is presented. Analysis and validation of the algorithm are based on real-world PMU data. The algorithm shows comparable or better performance compared to the conventional multi-signal Prony analysis.

## Acknowledgement

This research was funded in part by MISO Energy under project “System Identification Using PMU Data”.

## References

- [1] P. Kundur, N.J. Balu, M.G. Lauby, *Power System Stability and Control*, McGraw-hill New York, 1994, vol. 7.
- [2] H. Ma, A. Girgis, et al., Identification and tracking of harmonic sources in a power system using a Kalman filter, *IEEE Trans. Power Deliv.* 11 (3) (1996) 1659–1665.
- [3] L. Fan, Y. Wehbe, Extended kalman filtering based real-time dynamic state and parameter estimation using PMU data, *Electr. Power Syst. Res.* 103 (2013) 168–177.
- [4] H.G. Aghamolki, Z. Miao, L. Fan, W. Jiang, D. Manjure, Identification of synchronous generator model with frequency control using unscented Kalman filter, *Electr. Power Syst. Res.* 126 (2015) 45–55.
- [5] B. Mogharbel, L. Fan, Z. Miao, Least squares estimation-based synchronous generator parameter estimation using PMU data, in: *IEEE PES General Meeting*, 2015.
- [6] N. Zhou, J. Pierre, J. Hauer, Initial results in power system identification from injected probing signals using a subspace method, in: *Power and Energy Society General Meeting-Conversion and Delivery of Electrical Energy in the 21st Century*, 2008 IEEE, IEEE, 2008, pp. 1–1.
- [7] J.F. Hauer, C. Demeure, L. Scharf, Initial results in prony analysis of power system response signals, *IEEE Trans. Power Syst.* 5 (1) (1990) 80–89.
- [8] J. Hauer, Application of prony analysis to the determination of modal content and equivalent models for measured power system response, *IEEE Trans. Power Syst.* 6 (3) (1991) 1062–1068.
- [9] D. Trudnowski, J. Johnson, J. Hauer, Making prony analysis more accurate using multiple signals, *IEEE Trans. Power Syst.* 14 (1) (1999) 226–231.
- [10] N. Zhou, Z. Huang, F. Tuffner, J. Pierre, S. Jin, Automatic implementation of Prony analysis for electromechanical mode identification from phasor measurements, in: *Power and Energy Society General Meeting*, 2010 IEEE, IEEE, 2010, pp. 1–8.
- [11] N. Zhou, J.W. Pierre, D.J. Trudnowski, R.T. Guttromson, Robust RLS methods for online estimation of power system electromechanical modes, *IEEE Trans. Power Syst.* 22 (3) (2007) 1240–1249.
- [12] S. Nabavi, A. Chakraborty, A real-time distributed prony-based algorithm for modal estimation of power system oscillations, in: *American Control Conference (ACC)*, 2014, IEEE, 2014, pp. 729–734.
- [13] S. Nabavi, A. Chakraborty, Distributed estimation of inter-area oscillation modes in large power systems using alternating direction multiplier method, in: *PES General Meeting Conference & Exposition*, 2014 IEEE, IEEE, 2014, pp. 1–5.
- [14] S. Nabavi, J. Zhang, A. Chakraborty, Distributed optimization algorithms for wide-area oscillation monitoring in power systems using interregional pmu-pdc architectures, *IEEE Trans. Smart Grid* 6 (5) (2015) 2529–2538.
- [15] J.H. Chow, K.W. Cheung, A toolbox for power system dynamics and control engineering education and research, *IEEE Trans. Power Syst.* 7 (4) (1992) 1559–1564.
- [16] M. Dehghani, B. Shayanfard, A.R. Khayatian, PMU ranking based on singular value decomposition of dynamic stability matrix, *IEEE Trans. Power Syst.* 28 (3) (2013) 2263–2270.
- [17] L. Ljung, *System Identification*, Prentice Hall, 1999.
- [18] A. Nedic, A. Ozdaglar, Distributed subgradient methods for multi-agent optimization, *IEEE Trans. Autom. Control* 54 (1) (2009) 48–61.
- [19] D.P. Bertsekas, *Nonlinear Programming*, Athena Scientific, 1999.